THE JOURNAL OF BIOLOGICAL CHEMISTRY VOL. 286, NO. 15, pp. 13733–13740, April 15, 2011

$G\alpha_q$ Signal in Osteoblasts Is Inhibitory to the Osteoanabolic Action of Parathyroid Hormone*[S]

Received for publication, November 3, 2010, and in revised form, February 6, 2011 Published, JBC Papers in Press, February 23, 2011, DOI 10.1074/jbc.M110.200196

Naoshi Ogata[‡], Yusuke Shinoda[§], Nina Wettschureck[¶], Stefan Offermanns[¶], Shu Takeda[‖], Kozo Nakamura[§], Gino V. Segre[**], Ung-il Chung[‡‡], and Hiroshi Kawaguchi[§1]

From the Departments of [‡]Bone and Cartilage Regenerative Medicine and [§]Sensory and Motor System Medicine and the [‡‡]Center for Disease Biology and Integrative Medicine, University of Tokyo, Tokyo 113-8655, Japan, the [¶]Department of Pharmacology, Max-Planck-Institute for Heart and Lung Research, Ludwigstrasse 43, Bad Nauheim 61231, Germany, the [‖]Department of Endocrinology and Metabolism, School of Medicine, Keio University, Tokyo 160-8582, Japan, and the [**]Endocrine Unit, Massachusetts General Hospital, Harvard Medical School, Boston, Massachusetts 02114

This study examined the role of the $G\alpha_q$ signal constituted by $G\alpha_q$ and $G\alpha_{11}$ (encoded by *Gnα$_q$* and *Gnα$_{11}$*, respectively), a major intracellular pathway of parathyroid hormone (PTH), in the PTH osteoanabolic action by the gain- and loss-of-function analyses. Transgenic mice with osteoblast-specific overexpression of the constitutively active *Gnα$_q$* gene under the control of 2.3-kb type I collagen α1 chain (*Col1a1*) promoter exhibited osteopenia with decreased bone formation parameters and did not respond to the daily PTH treatment. We then established osteoblast-specific *Gnα$_q$* and *Gnα$_{11}$* double-knock-out (cDKO) mice by crossing the 2.3-kb *Col1a1* promoter-*Cre* recombinase transgenic mice and those with *Gnα$_q$* gene flanked with loxP and global ablation of *Gnα$_{11}$* (*Col1a1*-Cre$^{+/-}$;*Gna$_q^{fl/fl}$*;*Gna$_{11}^{-/-}$*) and found that the cDKO and single knock-out littermates of *Gnα$_q$* or *Gnα$_{11}$* exhibited normal bone volume and turnover under physiological conditions. With a daily injection of PTH, however, the cDKO mice, but not the single knock-out mice, showed higher bone volume and turnover than the wild-type littermates. Cultures of primary osteoblasts derived from cDKO and wild-type littermates confirmed enhancement of the PTH osteoanabolic action by the $G\alpha_q$ signal deficiency in a cell-autonomous mechanism, in association with the membrane translocation of protein kinase Cδ. This enhancement was reproduced by overexpression of regulator of G protein signaling-2, a $G\alpha_q$ signal inhibitor, in osteoblastic MC3T3-E1 cells. Hence, the $G\alpha_q$ signal plays an inhibitory role in the PTH osteoanabolic action, suggesting that its suppression may lead to a novel treatment in combination with PTH against osteoporosis.

Bone anabolic action of parathyroid hormone (PTH)[2] has attracted considerable clinical attention, and led to the approval of the recombinant human PTH (1–34) for osteoporosis treatment worldwide (1, 2). PTH is known to bind to the type 1 PTH/PTH-related peptide (PTHrP) receptor (PTH1R), a class II G protein-coupled receptor superfamily member (3, 4), in osteoblasts and causes activation of the two major signal pathways via the G protein α subunits $G\alpha_s$ and $G\alpha_q$ (encoded by *Gnα$_s$* and *Gnα$_q$*, respectively) (5). Although $G\alpha_s$ leads to activation of adenylyl cyclase and an increase of intracellular levels of cAMP, $G\alpha_q$ activates phospholipase C which results in activation of protein kinase C (PKC) and an increase of intracellular Ca^{2+} ($[Ca^{2+}]_i$) concentration (6). Accumulated evidence of the *Gnα$_s$* gene mutations in human bone disorders like fibrous dysplasia, McCune-Albright syndrome, and Albright hereditary osteodystrophy indicates the osteoanabolic role of the $G\alpha_s$ signal (7, 8). This was supported by a study on mice with osteoblast-specific *Gnα$_s$* deficiency showing an impairment of bone formation (9, 10). Transgenic mice overexpressing constitutively active *Pth1r* via the $G\alpha_s$ signal in osteoblasts exhibit increased trabecular bone formation (11), and several studies also support the crucial role of the $G\alpha_s$ signal in the PTH osteoanabolic action thorough stimulation of osteoblast differentiation (12). Contrarily, little has been known about the role of the $G\alpha_q$ signal in bone metabolism. Hence, the present study sought to clarify the involvement of the $G\alpha_q$ signal in the PTH osteoanabolic action by examining the effects of gain- and loss-of-functions of the signal in osteoblasts.

Recently, we created transgenic mice with osteoblast-specific overexpression of the constitutively active *Gnα$_q$* gene under the control of the 2.3-kb type I collagen α1 chain (*Col1a1*) promoter (*Col1a1-Gna$_q$*-tg mice) and found that the mice exhibited osteopenia in trabecular and cortical bones, indicating an inhibitory function of the $G\alpha_q$ signal in bone formation under physiological conditions without PTH stimulation (13). However, mice with global deletion of *Gnα$_q$* showed normal bone phenotype while exhibiting cerebellar ataxia and platelet dysfunction (14). This may be due to redundant functionality of $G\alpha_q$ and $G\alpha_{11}$ (encoded by *Gnα$_{11}$*), a $G\alpha_q$ subfamily member that also activates phospholipase C and may compensate for the $G\alpha_q$ insufficiency (15). Although global *Gna$_{11}$* defi-

* This work was supported by Grants-in-aid for Scientific Research 21390416, 22659267, and 22390286 from the Japanese Ministry of Education, Culture, Sports, Science, and Technology.

[S] The on-line version of this article (available at http://www.jbc.org) contains supplemental Figs. 1–3.

[1] To whom correspondence should be addressed: Sensory and Motor System Medicine, Faculty of Medicine, University of Tokyo, Hongo 7-3-1, Bunkyo, Tokyo 113-8655, Japan. Tel.: 81-33815-5411 (ext. 30473); Fax: 81-33818-4082; E-mail: kawaguchi-ort@h.u-tokyo.ac.jp.

[2] The abbreviations used are: PTH, parathyroid hormone; ALP, alkaline phosphatase; BMD, bone mineral density; cDKO, conditional double-knock-out; Col1a1, type I collagen α1 chain; IGF-I, insulin-like growth factor-I; IRS-1, insulin receptor substrate-1; PDE, phosphodiesterase; PMA, phorbol 12-myristate 13-acetate; pQCT, peripheral quantitative computed tomography; RANKL, receptor activator of NF-κB ligand; RGS, regulator of G protein signaling; tg, transgenic.

cient mice showed no abnormality in any organs (16), the global *Gna$_q$* and *Gna$_{11}$* double-knock-out mice were embryonically lethal due to cardiomyocyte hypoplasia (17). Hence, to avoid compensation by Gα$_{11}$ solely in bone, we established *Gnα$_q$* and *Gnα$_{11}$* double-knock-out mice with osteoblast-specific ablation of *Gnα$_q$* and global ablation of *Gnα$_{11}$* for the loss-of-function analysis of the Gα$_q$ signal.

Upon activation of G protein-coupled receptor, there are several proteins that modulate the G protein-mediated signals including regulator of G protein signaling (RGS) (18–20). Among >20 RGS family members, RGS2 is known to be a selective inhibitor of the Gα$_q$ signal via Gα$_q$ and Gα$_{11}$ (21, 22). Hence, we also examined the effects of gain- and loss-of-functions of RGS2 on the PTH osteoanabolic action.

EXPERIMENTAL PROCEDURES

Mice—The transgenic mice overexpressing the constitutively active *Gna$_q$* gene or *Cre* gene under the control of 2.3-kb *Col1a1* promoter (*Col1a1-Gna$_q$*-tg and *Col1a1-Cre$^{+/-}$*, respectively) were generated as previously described (13, 23). The osteoblast-specific *Gnα$_q$* and *Gnα$_{11}$* double-knock-out (cDKO) mice were generated by crossing the 2.3-kb *Col1a1* promoter-*Cre* mice above (*Col1a1-Cre$^{+/-}$*) and those with *Gnα$_q$* gene flanked with loxP (*Gna$_q^{fl/fl}$*) and global ablation of *Gnα$_{11}$* (*Gnα$_{11}^{-/-}$*) (24). Intercrosses between *Col1a1-Cre$^{+/-}$*; *Gna$_q^{+/fl}$*;*Gna$_{11}^{+/-}$* mice resulted in the generation of osteoblast-specific cDKO (*Col1a1-Cre$^{+/-}$*;*Gna$_q^{fl/fl}$*;*Gna$_{11}^{-/-}$*) and wild-type (*Col1a1-Cre$^{-/-}$*;*Gna$_q^{fl/fl}$*;*Gna$_{11}^{+/+}$*) as well as single-knock-out mice of either *Gnα$_q$* (*Col1a1-Cre$^{+/-}$*;*Gnα$_q^{fl/fl}$*; *Gnα$_{11}^{+/-}$*) or *Gnα$_{11}$* (*Col1a1-Cre$^{+/-}$*;*Gnα$_q^{+/fl}$*;*Gnα$_{11}^{-/-}$*). Genotyping for *Gna$_q$* and *Gna$_{11}$* alleles was performed as described previously (17). Mice were on a mixed genetic background with a predominant contribution of the C57BL6/N strain, and male littermates were compared in each experiment. For the PTH treatment, mice received either 80 μg of recombinant rat PTH (1–34) (Sigma-Aldrich) per kg of body weight or the vehicle (PBS; Sigma-Aldrich) by subcutaneous injection five times/week for 4 weeks beginning at 8 weeks of age. All experiments were performed according to the protocol approved by the Animal Care and Use Committee of the University of Tokyo.

Radiological Analyses—Plain radiographs were taken using a soft x-ray apparatus (CMB-2; SOFTEX), and the bone mineral density (BMD) was measured by dual energy x-ray absorptiometry using a bone mineral analyzer (PIXImus Densitometer; GE Medical Systems). Computed tomographic scanning of the femurs was performed using a composite x-ray analyzer (NX-CP-C80H-IL; Nittetsu ELEX Co.) and reconstructed into a three-dimensional feature by the volume-rending method (VIP-Station; Teijin System Technology). Trabecular density was measured using a peripheral quantitative computed tomography (pQCT) analyzer (XCT Research SA+; Stratec Medizintecnik GmbH) at the metaphysis 1.4 mm above the distal growth plate of femurs.

Histological Analyses—For toluidine blue staining, samples were fixed with 70% ethanol, embedded in methyl methacrylate, and sectioned in 5-μm slices. Histomorphometric analyses were performed as described in an area 1.2 mm long from 0.5 mm below the growth plate of the proximal tibias (25), according to the ASBMR nomenclature report (26). For double labeling of the mineralization front, mice were injected subcutaneously with 16 mg/kg body weight of calcein at 5 days and 1 day before sacrifice.

Cell Cultures—For primary osteoblasts, calvariae of neonatal WT and cDKO littermates were digested by 0.1% collagenase and 0.2% dispase five times, and cells were isolated by the last three digestions were combined as an osteoblast population. Mouse osteoblastic MC3T3-E1 cells were purchased from RIKEN Cell Bank (Tsukuba, Japan). Cells were cultured in α-minimal essential medium (α-MEM; Invitrogen) containing 10% FBS (HyClone Laboratories, Inc., Logan, UT). In osteoblast differentiation experiments, medium was supplemented with 50 μg/ml ascorbic acid and 10 mM β-glycerophosphate (Sigma-Aldrich). For the intermittent treatment with PTH or phorbol 12-myristate 13-acetate (PMA), the cells were exposed to the agent for the first 6 h in each incubation cycle of 48 h and then cultured in its absence during the remainder of the cycle (12).

Gene Transfection—To construct the adenovirus expressing green fluorescent protein (GFP) (Ax-*GFP*) and *Rgs2* (Ax-*Rgs2*), cDNA encoding *GFP* and *Rgs2* was excised and subcloned into an adenoviral vector using an AdenoX Expression System (Takara Bio, Shiga, Japan), according to the manufacturer's instructions. Adenoviruses were amplified in HEK293 cells and purified with an AdenoX Virus Purification Kit (Takara Bio). Ax-GFP and AX-*Rgs2* were transfected at 100 multiplicities of infection for 24 h to MC3T3-E1 cells.

Alkaline Phosphatase (ALP) Activity and Staining—For ALP activity measurement, primary osteoblasts or MC3T3-E1 cells adenovirally transfected with *GFP* or *Rgs2* were cultured in the medium above with or without 10 nM recombinant rat PTH (1–34) and 100 nM PMA (Cell Signaling Technology, Beverly, MA). After six cycles (12 days) of intermittent treatment with PTH or PMA as described above, the cells were sonicated in 10 mM Tris-HCl buffer (pH 8.0) containing 1 mM $MgCl_2$ and 0.5% Triton X-100, and ALP activity in the lysate was measured using an ALP kit (Wako Pure Chemical Industry, Ltd., Osaka, Japan). The protein content was determined using BCA protein assay reagent (Pierce). For ALP staining, cells were fixed in 70% ethanol and stained for 10 min with a solution containing 0.01% naphthol AS-MX phosphate, 1% *N*,*N*-dimethyl formamide, and 0.06% fast blue BB (Sigma-Aldrich).

Real-time Quantitative RT-PCR—For measurement of *Col1a1* and osteocalcin (encoded by *Bglap*) mRNA, primary osteoblasts from WT and cDKO mice or MC3T3-E1 cells adenovirally transfected with *GFP* or *Rgs2* underwent six cycles (12 days) of intermittent treatment with 10 nM PTH or the vehicle as described above. For measuring *Rgs2* mRNA, MC3T3-E1 cells were precultured in α-MEM/10% FBS and further cultured in the presence of 10 nM PTH for the indicated times. Total RNA was extracted with ISOGEN (Wako Pure Chemical), and an aliquot (1 μg) was reverse-transcribed using a PrimeScript RT reagent kit (Takara Bio). For RT-PCR, real-time PCR was performed on an ABI Prism 7000 Sequence Detection System (ABI) using QuantiTect SYBR Green PCR Master Mix (Qiagen, Tokyo), according to the manufacturer's instructions. All reactions were run in triplicate. A set of

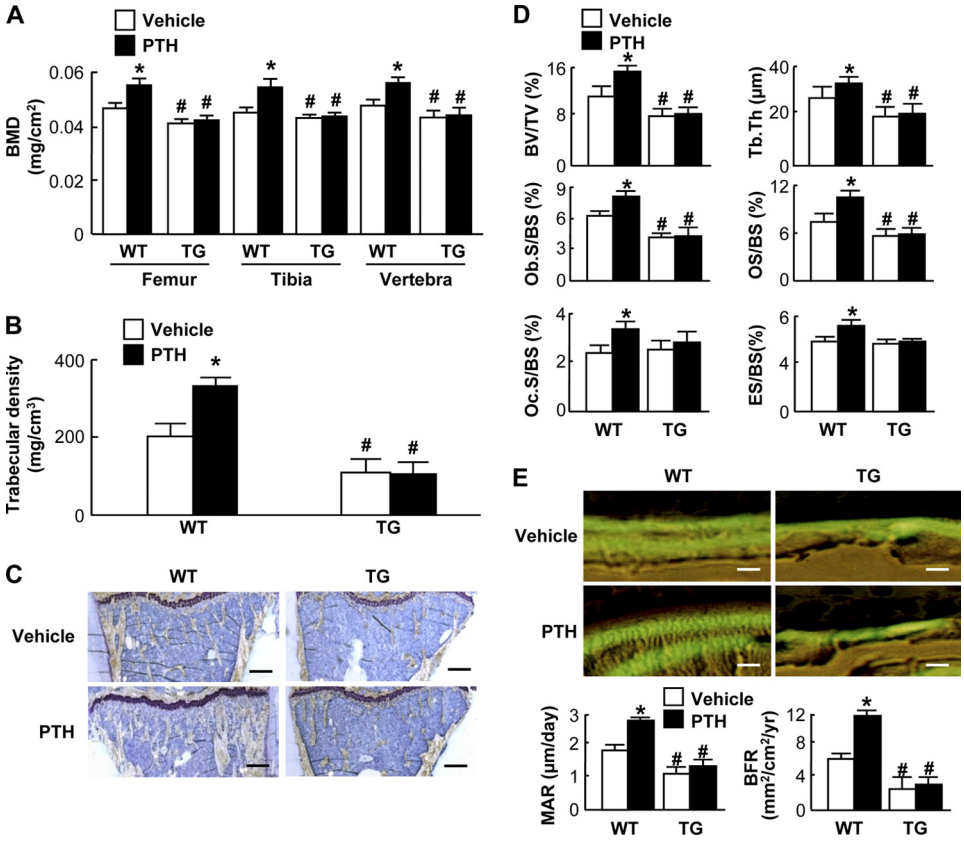

FIGURE 1. **Effects of daily PTH injection (80 μg/kg × 5 times × 4 weeks) on bones of 8-week-old *Col1a1-Gna$_q$*-tg (*TG*) and their wild-type (*WT*) littermates.** *A*, BMD determined by dual energy x-ray absorptiometry of the entire femurs, tibias, and L2–L5 vertebrae. *B*, trabecular density determined by pQCT of the distal metaphysis of the femurs. *C*, toluidine blue staining of proximal tibias (*scale bars*, 200 μm). *D*, static histomorphometric parameters in the proximal tibias. *BV/TV*, trabecular bone volume as a percentage of total volume; *Tb.Th*, trabecular thickness; *Ob.S/BS*, percentage of the bone surface covered by cuboidal osteoblasts; *OS/BS*, percentage of the bone surface covered with osteoid; *Oc.S/BS*, percentage of bone surface covered by mature osteoclasts; *ES/BS*, percentage of eroded surface. *E*, *top*, double labelings with calcein of trabecular bones in the proximal tibias imaged by fluorescent microscopy (*scale bars*, 20 μm). *E*, *bottom*, dynamic histomorphometric parameters based on the double labelings above. *MAR*, mineral apposition rate; *BFR*, bone formation rate. Data in all graphs (*A*, *B*, *D*, and *E*) are expressed as mean (*bars*) ± S.E. (*error bars*) for 4 mice/group. *, $p < 0.01$ *versus* vehicle; #, $p < 0.01$ *versus* WT.

primers was designed using sequences obtained from the GenBank as follows: 5′-ACGTCCTGGTGAAGTTGGTC-3′ and 5′-CAGGGAAGCCTCTTTCTCCT-3′ for *Col1a1* mRNA (U08020.1), 5′-AAGCAGGAGGGCAATAAGGT-3′ and 5′-TTTGTAGGCGGTCTTCAAGC-3′ for *Bglap* mRNA (NM007541.1), and 5′-CCGAGTTCTGTGAAGAAAAC-ATTG-3′ and 5′-GGGACTCCTGGTCTCATGTAGCAT-3′ for *Rgs2* mRNA (NP002914.1).

Immunoblotting and Immunoprecipitation—For the protein expressions of $G\alpha_q$ and $G\alpha_{11}$ in tissues, liver, heart, kidney, whole brain, femurs, and tibias from neonatal mice were homogenized in T-PER (Pierce Chemical) on ice using a 200-μl microtissue grinder (Wheaton, Millville, NJ). For long bones, as much surrounding soft tissue was removed as possible, and bones were immediately frozen in liquid nitrogen. Homogenates (25 μg of protein) were then subjected to SDS-PAGE. For the protein expression of PKCs, primary osteoblasts were treated with 10 nM PTH or vehicle for 30 min. The lysates of the whole cells and the cell membrane were prepared using an M-PER kit and a Mem-PER kit (Pierce Chemical) and were subjected to SDS-PAGE. Immunoblotting was performed using antibodies to common epitopes of $G\alpha_q$ and $G\alpha_{11}$, $G\alpha_s$, RGS2, PKCβI, PKCδ, PKCϵ, PKCη (a dilution of 1:1000; Cell Signaling Technology), and actin (1:1,000; Sigma-Aldrich), followed with horseradish peroxidase-conjugated goat anti-mouse IgG and goat anti-rabbit IgG (a dilution of 1:10,000; Amersham Biosciences). For immunoprecipitation, the whole cell lysates (500 μg of total protein) prepared using the M-PER kit were incubated with 2 μg of antibody to $G\alpha_s$ or the $G\alpha_q$/$G\alpha_{11}$ above using a Catch and Release kit (Upstate Biotechnology).

Measurements of Intracellular cAMP and $[Ca^{2+}]_i$—For the measurement of intracellular cAMP, the transfected cells were precultured in serum-free α-MEM containing 0.1% BSA and 1 mM 3-isobutyl-1-methylxanthine (Sigma-Aldrich) for 10 min and further cultured in the presence of 10 nM PTH at 37 °C for 15 min. The amount of cAMP in the cell extracts was determined by cAMP Biotrak EIA System (Amersham Biosciences). For the measurement of $[Ca^{2+}]_i$, transfected MC3T3-E1 cells were loaded with 4 μM fura-2 AM (Invitrogen) in physiological salt solution containing 150 mM NaCl, 4 mM KCl, 2 mM $CaCl_2$, 1 mM $MgCl_2$, 5.6 mM glucose, and 10 mM HEPES and were cultured in the presence of 10 nM PTH for 5 min. The excitation wavelengths of 345 nm and 380 nm were acquired using an inverted microscope (IX70; Olympus, Tokyo) equipped with a cooled charge-coupled device camera (Rolera XR, Qimaging, Canada). Image analysis was carried out using IPLab software (BD Biosciences Bioimaging, Rockville, MD).

Statistical Analyses—Means of groups were compared by ANOVA. Significance of differences was determined by post hoc testing with Bonferroni's method.

RESULTS

Effect of Osteoblast-specific Gnα$_q$ Overexpression on Osteoanabolic Action of PTH—To know the effect of the gain-of-function of Gα$_q$ signal on the osteoanabolic action of PTH, we initially used transgenic mice with overexpression of the constitutively active *Gnα$_q$* gene under the control of 2.3-kb type I collagen α1 chain promoter (*Col1a1-Gna$_q$*-tg). As we reported previously (13), the *Col1a1-Gna$_q$*-tg mice under the vehicle treatment exhibited radiographic and histologic osteopenia with decreases in static and dynamic histomorphometric parameters for bone formation compared with the wild-type littermates (Fig. 1). In wild-type mice, the daily injection of PTH for 4 weeks caused an increase in bone volume with enhancement of bone formation and resorption parameters compared with the vehicle treatment, consistent with previous reports by others and us (27–29). However, in transgenic mice, there were no significant differences between the vehicle and PTH treatment groups in bone volume or histomorphometric parameters, indicating that the gain-of-function of the Gα$_q$ signal in osteoblasts cancels the PTH osteoanabolic action.

Effect of Osteoblast-specific Gnα$_q$ and Gnα$_{11}$ Double-knock-out on Osteoanabolic Action of PTH—To explore further the role of endogenous Gα$_q$ signal in bone, we established conditional *Gnα$_q$* and *Gnα$_{11}$* double-knock-out (cDKO: *Col1a1-Cre$^{+/-}$;Gna$_q$$^{fl/fl}$;Gna$_{11}$$^{-/-}$*) mice with osteoblast-specific ablation of *Gnα$_q$* and global ablation of *Gnα$_{11}$* to avoid the compensation by the redundant functionality of Gα$_q$ and Gα$_{11}$. Initially, we looked at expression patterns of Gα$_q$ and Gα$_{11}$ proteins in various tissues of mice of four genotypes depending on deficiency of *Gnα$_q$* and *Gnα$_{11}$* genes: *Col1a1-Cre$^{-/-}$;Gnα$_q$$^{fl/fl}$;Gnα$_{11}$$^{+/+}$* (wild-type), *Col1a1-Cre$^{+/-}$;Gnα$_q$$^{fl/fl}$;Gnα$_{11}$$^{+/-}$*, *Col1a1-Cre$^{+/-}$;Gnα$_q$$^{+/fl}$;Gnα$_{11}$$^{-/-}$*, and *Col1a1-Cre$^{+/-}$;Gnα$_q$$^{fl/fl}$;Gnα$_{11}$$^{-/-}$* (cDKO). The cDKO mice were confirmed to show a specific defect of both Gα$_q$ and Gα$_{11}$ protein expressions in bone (Fig. 2*A*). These mice developed and grew normally without abnormality in major organs (Fig. 2*B*). In addition, there was no significant difference of bone shape or bone volume of the cDKO mice compared with the wild-type littermates or single-knock-out littermates of either *Gnα$_q$* (*Col1a1-Cre$^{+/-}$;Gnα$_q$$^{fl/fl}$;Gnα$_{11}$$^{+/-}$*) or *Gnα$_{11}$* (*Col1a1-Cre$^{+/-}$;Gnα$_q$$^{+/fl}$;Gnα$_{11}$$^{-/-}$*) under physiological conditions (Fig. 2*C* and supplemental Fig. 1).

To know the effect of loss-of-function of the Gα$_q$ signal on the PTH osteoanabolic action, we administered daily PTH injections to mice of the four genotypes and compared the bone volume and turnover. Under the vehicle treatment, there was no significant difference among genotypes in BMD (Fig. 3, *A* and B), trabecular density (Fig. 3*C*), or histomorphometric parameters for bone formation and resorption in either trabecular or cortical bones (Fig. 3, *D*–*F*). Here again, the daily PTH treatment was confirmed to cause increases in bone volume, bone formation, and resorption parameters in the wild-type mice. These effects of PTH on bone volume and turnover were more greatly increased in the cDKO mice than in the wild-type littermates, although not in single-knock-out mice of either *Gnα$_q$* or *Gnα$_{11}$*. These indicate that the loss-of-function of the Gα$_q$ signal in osteoblasts enhances the osteoanabolic actions of PTH.

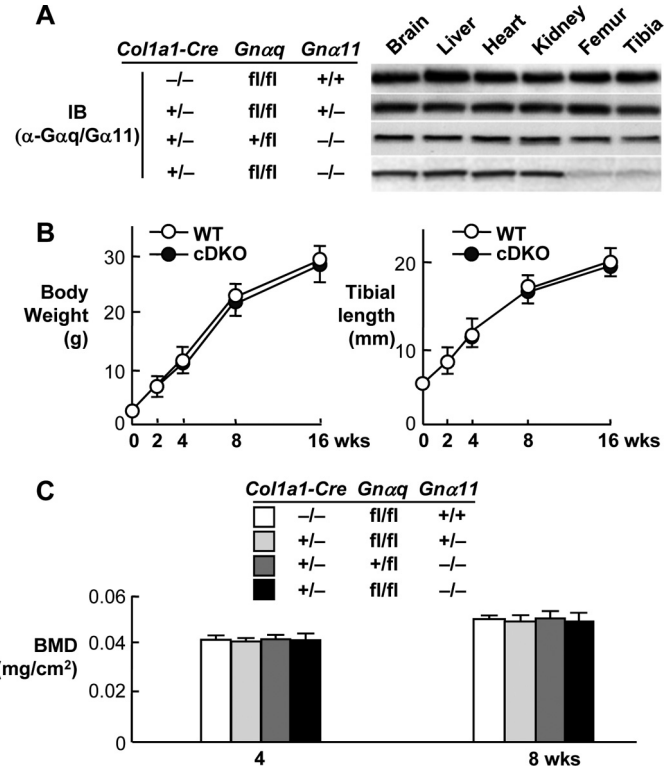

FIGURE 2. **Phenotypes of *Col1a1-Cre$^{+/-}$;Gna$_q$$^{fl/fl}$;Gna$_{11}$$^{-/-}$* (cDKO) mice under physiological conditions.** *A*, expression patterns of Gα$_q$ and Gα$_{11}$ proteins by Western blotting using an antibody to common epitopes of Gα$_q$ and Gα$_{11}$ (α-Gα$_q$/Gα$_{11}$) in several tissues of neonatal mice of four genotypes depending on deficiency of *Gnα$_q$* and *Gnα$_{11}$* genes: *Col1a1-Cre$^{-/-}$;Gnα$_q$$^{fl/fl}$;Gnα$_{11}$$^{+/+}$* (*WT*), *Col1a1-Cre$^{+/-}$;Gnα$_q$$^{fl/fl}$;Gnα$_{11}$$^{+/-}$*, *Col1a1-Cre$^{+/-}$;Gnα$_q$$^{+/fl}$;Gnα$_{11}$$^{-/-}$*, and *Col1a1-Cre$^{+/-}$;Gnα$_q$$^{fl/fl}$;Gnα$_{11}$$^{-/-}$* (cDKO). *B*, body weight (*left*) and tibial length (*right*) of the WT and cDKO littermates at the indicated ages. Data are expressed as means (*symbols*) ± S.E. (*error bars*) for 4 or 5 mice/group per time. There were no significant differences between genotypes at any time points. *C*, BMD determined by dual energy x-ray absorptiometry of the entire tibias of mice of four genotypes above at 4 and 8 weeks of age. Data are expressed as mean (*bars*) ± S.E. (*error bars*) for 3–5 mice/group per time. There were no significant differences among genotypes.

We then compared cultures of primary calvarial osteoblasts derived from cDKO mice with those from wild-type littermates. Intermittent treatment of PTH stimulated differentiation and matrix synthesis of cultured osteoblasts determined by ALP activity and mRNA levels of osteogenesis markers such as *Col1a1* and *Bglap*, and the PTH effects were enhanced in the cultures of cDKO osteoblasts compared with the wild-type cultures, indicating that loss-of-function effect of the Gα$_q$ signal on the PTH osteoanabolic action was cell-autonomous in osteoblasts (Fig. 4*A*). The enhancement of the PTH effect in the cDKO cells was inhibited by addition of PMA, a PKC activator, suggesting that PKC normally retards the PTH effects (Fig. 4*B*).

Hence, we looked at protein levels of PKC isoforms that are known to be expressed in osteoblasts: PKCβI, PKCδ, PKCε, and PKCη (30), in primary osteoblasts from the two genotypes cultured with and without PTH. Neither PTH treatment nor the Gα$_q$ signal deficiency altered any PKC isoform levels in the

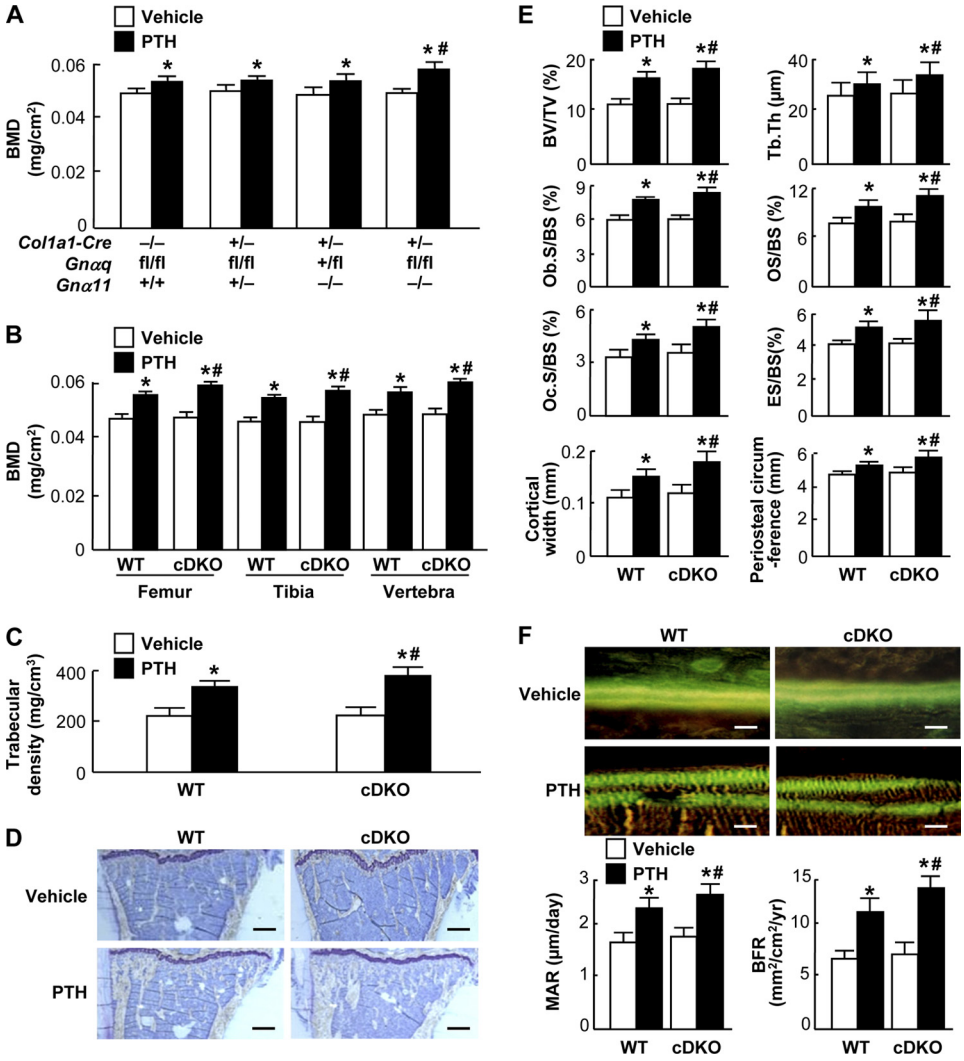

FIGURE 3. **Effects of daily PTH injection (80 μg/kg × 5 times × 4 weeks) on bones of 8-week-old *Col1a1-Cre*$^{+/-}$;*Gnα$_q$*$^{fl/fl}$;*Gnα$_{11}$*$^{-/-}$ (cDKO) and the wild-type (*WT*: *Col1a1-Cre*$^{-/-}$;*Gnα$_q$*$^{fl/fl}$;*Gnα$_{11}$*$^{+/+}$) littermates.** *A*, BMD determined by dual energy x-ray absorptiometry of the entire tibias of mice of four genotypes: WT, two single-knock-out mice (*Col1a1-Cre*$^{+/-}$;*Gnα$_q$*$^{fl/fl}$;*Gnα$_{11}$*$^{+/-}$ and *Col1a1-Cre*$^{+/-}$;*Gnα$_q$*$^{+/fl}$;*Gnα$_{11}$*$^{-/-}$), and cDKO. *B*, BMD of the entire femurs, tibias, and L2–L5 vertebrae. *C*, trabecular density determined by pQCT of the distal metaphysis of the femurs. *D*, toluidine blue staining of proximal tibias (*scale bars*, 200 μm). *E*, static histomorphometric parameters in the proximal tibias as shown in Fig. 1*D*, and cortical bone parameters (*two bottom graphs*). *F*, *top*, double labelings with calcein of trabecular bones in the proximal tibias imaged by fluorescent microscopy (*scale bars*, 20 μm). *F*, *bottom*, dynamic histomorphometric parameters based on the double labelings above as shown in Fig. 1*E*. Data in all graphs (*A*, *B*, *C*, *E*, and *F*) are expressed as mean (*bars*) ± S.E. (*error bars*) for 4 or 5 mice/group. *, $p < 0.01$ *versus* vehicle; #, $p < 0.01$ *versus* WT with PTH treatment.

whole cell lysates, suggesting that there was no regulation of the PKC isozyme expressions. In the membrane extracts of wild-type osteoblasts, however, only PKCδ level was increased by PTH treatment, and this stimulation was suppressed in the cDKO osteoblasts, implicating that membrane translocation of PKCδ by PTH may be associated with the Gα$_q$ signal (Fig. 4*C*). Taken together, these *in vivo* and *ex vivo* results demonstrate the inhibitory role of the Gα$_q$ signal in osteoblasts, possibly in association with the PKCδ membrane translocation, in the osteoanabolic action of PTH.

Involvement of RGS2 in the PTH Osteoanabolic Action—We next examined the involvement of RGS2, a putative inhibitor of the Gα$_q$ signal (21, 22), in the PTH osteoanabolic action. The *Rgs2* expression was increased in response to PTH treatment in cultured osteoblastic MC3T3-E1 cells (Fig. 5*A*). Immunoprecipitation/immunoblotting analyses confirmed the physical interaction of RGS2 with Gα$_q$/Gα$_{11}$ protein, but not with Gα$_s$ protein, after the PTH treatment (Fig. 5*B*). Adenoviral overexpression of *Rgs2* caused partial but significant suppression of intracellular Ca^{2+} elevation, but not cAMP accumulation, by the PTH treatment in MC3T3-E1 cells (Fig. 5*C*). These confirm that RGS2 binds directly to Gα$_q$/Gα$_{11}$ protein and partially inhibits the Gα$_q$ signal without affecting the Gα$_s$ signal. The *Rgs2* overexpression enhanced the stimulation of *Col1a1* expression and ALP activity by intermittent treatment with PTH in MC3T3-E1 cells (Fig. 5*D*), just as the genetic deficiency of the Gα$_q$ signal did in primary osteoblasts. Again, the enhancement of the PTH effect by the *Rgs2* overexpression was inhibited by addition of PMA, suggesting that PKC retards the PTH effects (Fig. 5*E*).

DISCUSSION

The present gain- and loss-of-function analyses in *Col1a1-Gna$_q$*-tg mice and *Col1a1-Cre*$^{+/-}$;*Gna$_q$*$^{fl/fl}$;*Gna$_{11}$*$^{-/-}$ mice,

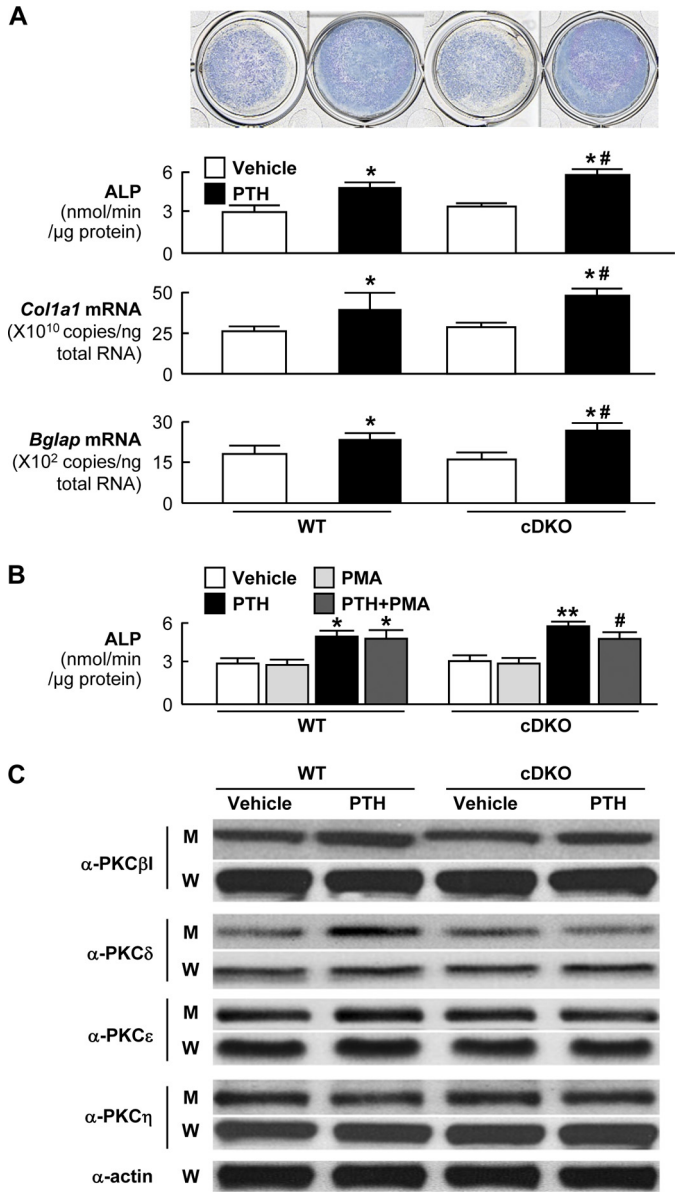

FIGURE 4. **Primary cultures of osteoblasts from neonatal calvariae of *Col1a1-Cre*$^{+/-}$;*Gnα$_q$*$^{fl/fl}$;*Gnα$_{11}$*$^{-/-}$ (cDKO) and the wild-type (*WT*: *Col1a1-Cre*$^{-/-}$;*Gnα$_q$*$^{fl/fl}$;*Gnα$_{11}$*$^{+/+}$) littermates.** *A*, ALP staining and activity (*upper two rows*) and mRNA levels of *Col1a1* and osteocalcin (encoded by *Bglap*) (*lower two rows*) after six cycles (12 days) of intermittent treatment with and without 10 nM PTH. *, $p < 0.01$ *versus* vehicle; #, $p < 0.01$ *versus* WT with PTH treatment. *B*, ALP activity after the intermittent treatment above with and without PTH or PMA. *, $p < 0.01$ *versus* WT with vehicle; **, $p < 0.01$ *versus* WT with PTH; #, $p < 0.05$ *versus* cDKO with PTH alone. *C*, protein levels of PKC isoforms determined by immunoblotting using respective antibodies (α-*PKCs*) in the membrane extracts (*M*) and whole cell lysates (*W*) of primary osteoblasts from two genotypes cultured with and without PTH for 30 min. Data in all graphs (*A* and *B*) are expressed as mean (*bars*) ± S.E. (*error bars*) for 5 cultures/group.

respectively, demonstrated the inhibitory role of the Gα$_q$ signal in the PTH osteoanabolic action (Fig. 5*F*). Although this suggests that suppression of the signal may lead to a novel treatment in combination with PTH against osteoporosis, there is no agent or drug that directly suppresses the Gα$_q$ signal. Hence, we focused on RGS2, a physiological inhibitor of the Gα$_q$ signal, and found that the *Rgs2* overexpression enhanced the PTH osteoanabolic action in cultured osteoblasts. The RGS2 expression is known to be stimulated by phosphodiesterase (PDE) inhibitors which are now clinically used for treatment of erectile dysfunction, asthma, and pulmonary arterial hypertension (31). In fact, our preliminary examination confirmed that PDE6, a PDE family member, was expressed in MC3T3-E1 cells and primary mouse calvarial osteoblasts (supplemental Fig. 2*A*). When MC3T3-E1 cells were treated with zaprinast, a PDE6 inhibitor that is now clinically used as a drug for pulmonary arterial hypertension, the *Rgs2* expression was significantly up-regulated (supplemental Fig. 2*B*). Hence, we speculate that PDE inhibitors might possibly be useful for clinical application to osteoporosis treatment as an enhancer of the PTH osteoanabolic action via the RGS2 induction and the Gα$_q$ suppression.

To know the *in vivo* function of RGS2 on bone, our preliminary study compared BMD between mice with global deletion of *Rgs2* (*Rgs2*$^{-/-}$) and the wild-type littermates. Unlike *Col1a1-Gna$_q$*-tg mice that exhibited osteopenia with and without PTH treatment (Fig. 1), there was no significant difference in BMD between *Rgs2*$^{-/-}$ and wild-type littermates either with or without the treatment (supplemental Fig. 3*A*). This may possibly be due to insufficient activation of the Gα$_q$ signal by the *Rgs2* deficiency, as suggested by only a partial inhibition of the intracellular Ca^{2+} elevation by the *Rgs2* overexpression (Fig. 5*C*). In fact, primary osteoblasts derived from *Rgs2*$^{-/-}$ mice showed Ca^{2+} elevation under the PTH treatment similar to that from WT mice, whereas *Col1a1-Gna$_q$*-tg osteoblasts exhibited enhanced Ca^{2+} elevation (supplemental Fig. 3*B*). Alternatively, because RGS2 is generally deficient in the global *Rgs2*$^{-/-}$ mice, possible involvement of systemic regulation by the Gα$_q$ signal activation in other organs cannot be ruled out. For example, cardiac hypertrophy caused by the myocardial Gα$_q$ activation in the *Rgs2*$^{-/-}$ mice (32) may enhance the general blood flow, causing an increase of circulation in bone tissue. Hence, examination of PTH osteoanabolic action using conditional knock-out mice of *Rgs2* will be the next task for us to elucidate the function of RGS2 in bone.

The PTH osteoanabolic action was enhanced only in the cDKO mice, but not in single-knock-out mice of either *Gnα$_q$* or *Gnα$_{11}$*, confirming a redundant functionality of Gα$_q$ and Gα$_{11}$ in osteoblasts (Fig. 3). To date, no human diseases have been attributed to mutations in the *Gnα$_q$* gene. The lack of syndromes caused by loss-of-function mutations is readily understood because of the redundant functionality, making it necessary to have simultaneous mutations in both genes (17). The absence of a syndrome because of a dominant-acting mutation is less apparent. Mice with global *Gna$_q$* and *Gna$_{11}$* double-knock-out were embryonically lethal due to cardiomyocyte hypoplasia (17), and those with parathyroid-specific double-knock-out exhibited a phenotype resembling germ line knock-out of the extracellular Ca^{2+}-sensing receptor: severe hypercalcemia, hyperparathyroidism, hypocalciuria, growth retardation, and early postnatal death (33). Hence, Gα$_q$ and Gα$_{11}$ may compensate each other's function in various tissues.

Although *Gnα$_q$* transgenic mice in this study showed severe osteopenia (Fig. 1), no significant phenotype was observed in the cDKO mice under physiological conditions (Fig. 2). Simi-

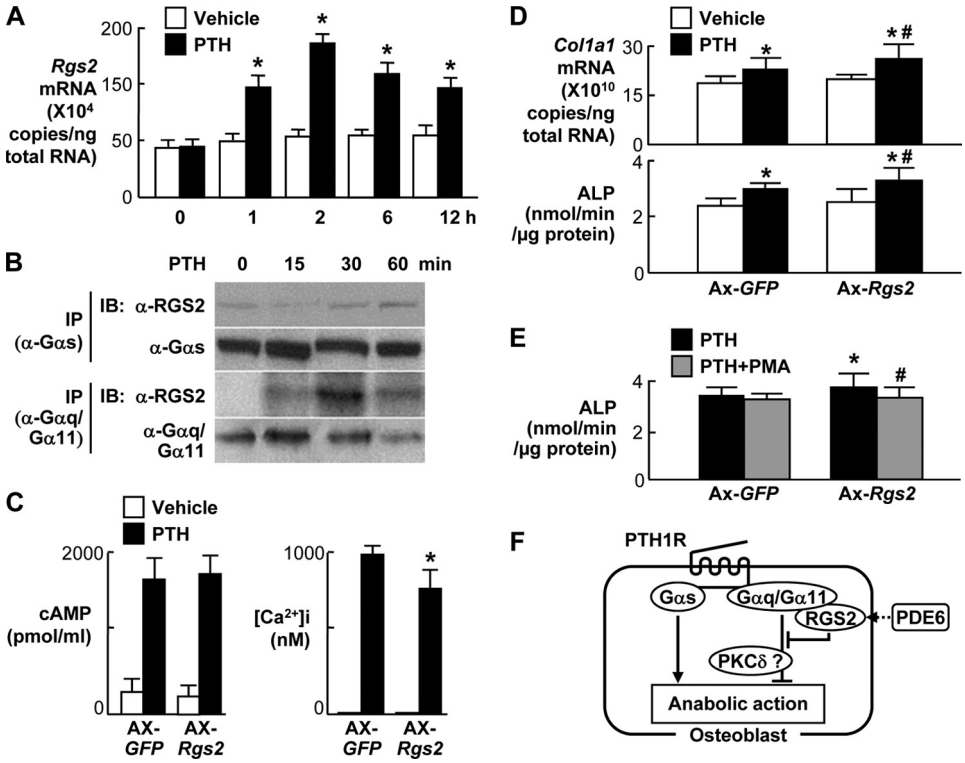

FIGURE 5. **Involvement of RGS2 in the PTH (10 nM) action on osteoblastic MC3T3-E1 cells.** *A*, time course of the *Rgs2* mRNA level by real-time RT-PCR in MC3T3-E1 cells cultured with and without PTH. *, $p < 0.01$ *versus* vehicle. *B*, time course of protein bindings of RGS2 with $G\alpha_s$ and $G\alpha_q/G\alpha_{11}$ after PTH treatment by immunoprecipitation (*IP*)/immunoblotting (*IB*) analyses using respective antibodies to RGS2 and $G\alpha_s$ (α-RGS2 and α-$G\alpha_s$) or an antibody to common epitopes of $G\alpha_q$ and $G\alpha_{11}$ (α-$G\alpha_q/G\alpha_{11}$). *C*, intracellular cAMP accumulation and Ca^{2+} ($[Ca^{2+}]_i$) concentration in MC3T3-E1 cells with adenoviral overexpression of *Rgs2* (Ax-*Rgs2*) or the control vector (Ax-*GFP*) after 15 min and 5 min treatment, respectively, with and without PTH. *, $p < 0.01$ *versus* Ax-*GFP*. *D*, *Col1a1* mRNA level and ALP activity in MC3T3-E1 cells with adenoviral overexpression of *Rgs2* (Ax-*Rgs2*) or the control vector (Ax-*GFP*) after six cycles (12 days) of intermittent treatment with and without PTH. *, $p < 0.01$ *versus* vehicle; #, $p < 0.01$ *versus* Ax-*GFP* with PTH treatment. *E*, ALP activity after the intermittent PTH treatment above with and without PMA. *, $p < 0.05$ *versus* Ax-*GFP* without PMA; #, $p < 0.05$ *versus* Ax-*Rgs2* without PMA. Data in all graphs (*A*, *C*, *D*, and *E*) are expressed as mean (*bars*) ± S.E. (*error bars*) for five cultures/group. *F*, schematic of effects of $G\alpha_s$ and $G\alpha_q$ signals in osteoblasts on the PTH osteoanabolic action.

larly, in cultures without PTH treatment, osteoblasts from the transgenic mice showed an increase of PKC activity and decreases in differentiation markers in our previous study (13), whereas osteoblasts from the cDKO mice showed normal PKC activity and differentiation markers (Fig. 4). This is consistent with findings of cardiomyocyte-specific *Gna$_q$* and *Gna$_{11}$* double-knock-out mice that showed no cardiac abnormality under physiological conditions but showed a lack of ventricular hypertrophy in response to pressure overload (24). These indicate the existence of other compensatory mechanisms for the $G\alpha_q$ signal deficiency under physiological conditions, which became insufficient under pathological conditions like PTH stimulation or pressure overload.

There was no significant difference between WT and *Col1a1-Gna$_q$*-tg in resorption parameters (Oc.S/BS and ES/BS) under the PTH stimulation ($p > 0.05$) (Fig. 1*D*). This is consistent with our previous results on *ex vivo* analyses of cultured osteoblasts derived from the WT and *Col1a1-Gna$_q$*-tg mice, which show no difference in mRNA level of RANKL or osteoprotegerin, nor in the RANKL/osteoprotegerin ratio between WT and *Col1a1-Gna$_q$*-tg osteoblasts under the PTH treatment (13), implicating involvement of the $G\alpha_q$ signal in the PTH anabolic action rather than in the catabolic action. However, these resorption parameters under the PTH treatment were enhanced in the cDKO mice (Fig. 3*E*). Although we assume that this catabolic effect may be secondary to the anabolic effect via the coupling between bone formation and resorption, we cannot deny the possibility of direct involvement of the $G\alpha_q$ signal in the PTH catabolic action. Further studies using a model of continuous infusion of PTH by implanting a minipump, instead of the daily and intermittent injection used in the present study, will be needed to answer the question.

The present study used 8-week-old mice, which may seem somewhat young for the experiment of PTH that is indicated for osteoporosis treatment in humans. However, little is known about the age-related osteoanabolic action of PTH in mice. A previous study showed that it is variable depending on the site: in the tibia and femur it is nearly twice as great in young mice as it is in aged mice, whereas in the vertebra it is greater in aged mice (34). Because the present study performed bone analyses mainly in the tibia and femur, we used 8-week-old mice to increase the sensitivity of the assay. Similar analyses in the vertebra of 4–6-month-old mice may add further information for the application to the treatment of osteoporosis in humans.

Previous studies by others and us have shown that insulin-like growth factor (IGF)-I and its signaling molecule insulin-receptor substrate (IRS)-1 at least partly mediate the PTH osteoanabolic action (12, 27, 35, 36). However, PTH is reported to induce IGF-I expression via the cAMP accumulation through the $G\alpha_s$ signal (37, 38). In fact, our analyses revealed that IGF-I concentrations in the serum of *Col1a1-Gna$_q$*-tg and cDKO mice were comparable with those of respective wild-type

littermates and that the concentration in the culture medium of cDKO osteoblasts was similar to that of the wild-type cultures (data not shown), denying involvement of the Gα$_q$ signal in the IGF-I production. Hence, the Gα$_q$ signal might possibly affect the intracellular signal lying downstream of the IGF-I receptor like IRS-1/Akt pathway as reported in the process of cardiac hypertrophy and keratinocyte migration (39, 40). Another candidate for the mediator of the PTH osteoanabolic action is sclerostin, an endogenous inhibitor of the Wnt signal (41). However, this signal is also dependent on the Gα$_s$/cAMP pathway (42). So far, there are many other molecules like IL-18, β-arrestin2, connexin43, TGF-β, ATF-4, and CREM, which have been suggested to be involved in the PTH osteoanabolic action using their knock-out mice (43, 44). Moreover, *in vitro* screenings identified c-fos, RUNX2, and cAMP response element binding-protein as downstream molecules of PTH in osteoblasts (45). However, none of these molecules has been shown to be linked to the Gα$_q$ signal in the process of the PTH osteoanabolic action thus far. Elucidation of the molecular network related to the Gα$_q$ signal is anticipated to lead to a novel treatment in combination with PTH against osteoporosis.

Acknowledgments—We thank R. Yamaguchi and H. Kawahara for technical assistance.

REFERENCES

1. Neer, R. M., Arnaud, C. D., Zanchetta, J. R., Prince, R., Gaich, G. A., Reginster, J. Y., Hodsman, A. B., Eriksen, E. F., Ish-Shalom, S., Genant, H. K., Wang, O., and Mitlak, B. H. (2001) *N. Engl. J. Med.* **344,** 1434–1441
2. Hodsman, A. B., Bauer, D. C., Dempster, D. W., Dian, L., Hanley, D. A., Harris, S. T., Kendler, D. L., McClung, M. R., Miller, P. D., Olszynski, W. P., Orwoll, E., and Yuen, C. K. (2005) *Endocr. Rev.* **26,** 688–703
3. Jüppner, H., Abou-Samra, A. B., Freeman, M., Kong, X. F., Schipani, E., Richards, J., Kolakowski, L. F., Jr., Hock, J., Potts, J. T., Jr., Kronenberg, H. M., *et al.* (1991) *Science* **254,** 1024–1026
4. Abou-Samra, A. B., Jüppner, H., Force, T., Freeman, M. W., Kong, X. F., Schipani, E., Urena, P., Richards, J., Bonventre, J. V., and Potts, J. T., Jr. (1992) *Proc. Natl. Acad. Sci. U.S.A.* **89,** 2732–2736
5. Datta, N. S., and Abou-Samra, A. B. (2009) *Cell. Signal.* **21,** 1245–1254
6. McCudden, C. R., Hains, M. D., Kimple, R. J., Siderovski, D. P., and Willard, F. S. (2005) *Cell. Mol. Life Sci.* **62,** 551–577
7. Spiegel, A. M. (1997) *Horm. Res.* **47,** 89–96
8. Weinstein, L. S., Yu, S., Warner, D. R., and Liu, J. (2001) *Endocr. Rev.* **22,** 675–705
9. Sakamoto, A., Chen, M., Nakamura, T., Xie, T., Karsenty, G., and Weinstein, L. S. (2005) *J. Biol. Chem.* **280,** 21369–21375
10. Kronenberg, H. M. (2010) *Ann. N.Y. Acad. Sci.* **1192,** 327–329
11. Calvi, L. M., Sims, N. A., Hunzelman, J. L., Knight, M. C., Giovannetti, A., Saxton, J. M., Kronenberg, H. M., Baron, R., and Schipani, E. (2001) *J. Clin. Invest.* **107,** 277–286
12. Ishizuya, T., Yokose, S., Hori, M., Noda, T., Suda, T., Yoshiki, S., and Yamaguchi, A. (1997) *J. Clin. Invest.* **99,** 2961–2970
13. Ogata, N., Kawaguchi, H., Chung, U. I., Roth, S. I., and Segre, G. V. (2007) *J. Biol. Chem.* **282,** 35757–35764
14. Offermanns, S., Toombs, C. F., Hu, Y. H., and Simon, M. I. (1997) *Nature* **389,** 183–186
15. Gudermann, T., Kalkbrenner, F., and Schultz, G. (1996) *Annu. Rev. Pharmacol. Toxicol.* **36,** 429–459
16. Wettschureck, N., Moers, A., and Offermanns, S. (2004) *Pharmacol. Ther.* **101,** 75–89
17. Offermanns, S., Zhao, L. P., Gohla, A., Sarosi, I., Simon, M. I., and Wilkie, T. M. (1998) *EMBO J.* **17,** 4304–4312
18. De Vries, L., Zheng, B., Fischer, T., Elenko, E., and Farquhar, M. G. (2000) *Annu. Rev. Pharmacol. Toxicol.* **40,** 235–271
19. Ross, E. M., and Wilkie, T. M. (2000) *Annu. Rev. Biochem.* **69,** 795–827
20. Dromey, J. R., and Pfleger, K. D. (2008) *Endocr. Metab. Immune Disord. Drug Targets* **8,** 51–61
21. Zou, M. X., Roy, A. A., Zhao, Q., Kirshenbaum, L. A., Karmazyn, M., and Chidiac, P. (2006) *Cell. Signal.* **18,** 1655–1663
22. Hao, J., Michalek, C., Zhang, W., Zhu, M., Xu, X., and Mende, U. (2006) *J. Mol. Cell. Cardiol.* **41,** 51–61
23. Dacquin, R., Starbuck, M., Schinke, T., and Karsenty, G. (2002) *Dev. Dyn.* **224,** 245–251
24. Wettschureck, N., Rütten, H., Zywietz, A., Gehring, D., Wilkie, T. M., Chen, J., Chien, K. R., and Offermanns, S. (2001) *Nat. Med.* **7,** 1236–1240
25. Yamada, T., Kawano, H., Koshizuka, Y., Fukuda, T., Yoshimura, K., Kamekura, S., Saito, T., Ikeda, T., Kawasaki, Y., Azuma, Y., Ikegawa, S., Hoshi, K., Chung, U. I., Nakamura, K., Kato, S., and Kawaguchi, H. (2006) *Nat. Med.* **12,** 665–670
26. Parfitt, A. M., Drezner, M. K., Glorieux, F. H., Kanis, J. A., Malluche, H., Meunier, P. J., Ott, S. M., and Recker, R. R. (1987) *J. Bone Miner. Res.* **2,** 595–610
27. Bikle, D. D., Sakata, T., Leary, C., Elalieh, H., Ginzinger, D., Rosen, C. J., Beamer, W., Majumdar, S., and Halloran, B. P. (2002) *J. Bone Miner. Res.* **17,** 1570–1578
28. Yamaguchi, M., Ogata, N., Shinoda, Y., Akune, T., Kamekura, S., Terauchi, Y., Kadowaki, T., Hoshi, K., Chung, U. I., Nakamura, K., and Kawaguchi, H. (2005) *Endocrinology* **146,** 2620–2628
29. Kawano, T., Troiano, N., Adams, D. J., Wu, J. J., Sun, B. H., and Insogna, K. (2008) *Endocrinology* **149,** 4009–4015
30. Lampasso, J. D., Chen, W., and Marzec, N. (2006) *Int. J. Mol. Med.* **17,** 1125–1131
31. Bender, A. T., and Beavo, J. A. (2006) *Pharmacol. Rev.* **58,** 488–520
32. Takimoto, E., Koitabashi, N., Hsu, S., Ketner, E. A., Zhang, M., Nagayama, T., Bedja, D., Gabrielson, K. L., Blanton, R., Siderovski, D. P., Mendelsohn, M. E., and Kass, D. A. (2009) *J. Clin. Invest.* **119,** 408–420
33. Wettschureck, N., Lee, E., Libutti, S. K., Offermanns, S., Robey, P. G., and Spiegel, A. M. (2007) *Mol. Endocrinol.* **21,** 274–280
34. Knopp, E., Troiano, N., Bouxsein, M., Sun, B. H., Lostritto, K., Gundberg, C., Dziura, J., and Insogna, K. (2005) *Endocrinology* **146,** 1983–1990
35. Canalis, E., Centrella, M., Burch, W., and McCarthy, T. L. (1989) *J. Clin. Invest.* **83,** 60–65
36. Shinoda, Y., Kawaguchi, H., Higashikawa, A., Hirata, M., Miura, T., Saito, T., Nakamura, K., Chung, U. I., and Ogata, N. (2010) *J. Cell. Biochem.* **109,** 755–763
37. Umayahara, Y., Billiard, J., Ji, C., Centrella, M., McCarthy, T. L., and Rotwein, P. (1999) *J. Biol. Chem.* **274,** 10609–10617
38. Chang, W., Rewari, A., Centrella, M., and McCarthy, T. L. (2004) *J. Biol. Chem.* **279,** 42438–42444
39. Dorn, G. W., 2nd, and Force, T. (2005) *J. Clin. Invest.* **115,** 527–537
40. Taboubi, S., Garrouste, F., Parat, F., Pommier, G., Faure, E., Monferran, S., Kovacic, H., and Lehmann, M. (2010) *Mol. Biol. Cell* **21,** 946–955
41. Keller, H., and Kneissel, M. (2005) *Bone* **37,** 148–158
42. Bellido, T. (2006) *J. Musculoskelet. Neuronal Interact.* **6,** 358–359
43. Partridge, N. C., Li, X., and Qin, L. (2006) *Ann. N.Y. Acad. Sci.* **1068,** 187–193
44. Qiu, T., Wu, X., Zhang, F., Clemens, T. L., Wan, M., and Cao, X. (2010) *Nat. Cell Biol.* **12,** 224–234
45. Swarthout, J. T., D'Alonzo, R. C., Selvamurugan, N., and Partridge, N. C. (2002) *Gene* **282,** 1–17